Available online at www.sciencedirect.com
SCIENCE DIRECT®
Pergamon
Materials Research Bulletin 38 (2003) 1695–1703
Materials Research Bulletin
www.elsevier.com/locate/matresbu

# Sol–gel synthesis and characterization of mesoporous manganese oxide

Xinlin Hong[a], Gaoyong Zhang[a,b,*], Yinyan Zhu[a], Hengquan Yang[a]

[a]*School of Chemistry and Molecular Science, Wuhan University, Wuhan 430072, PR China*
[b]*China Research Institute of Daily Chemical Industry, Wenyuan Street No. 34, Taiyuan 030001, PR China*

Received 6 December 2002; received in revised form 2 July 2003; accepted 23 July 2003

**Abstract**

Mesoporous manganese oxide (MPMO) from reduction of $KMnO_4$ with maleic acid, was obtained and characterized in detail. The characterization of the material was confirmed by high-resolution transmission electron microscopy (HRTEM), X-ray powder diffractometry (XRD) and $N_2$ sorptometry. The results showed that MPMO is a pseudo-crystalline material with complex network pore structure, of which BET specific surface area is 297 $m^2/g$ and pore size distribution is approximately in the range of 0.7–6.0 nm. The MPMO material turns to cryptomelane when the calcinating temperature rises to 400 °C. The optimum sol–gel reaction conditions are $KMnO_4/C_4H_4O_4$ molar ratio = 3, pH = 7 and gelation time > 6 h.


*Keywords:* A. Oxides; B. Sol–gel synthesis

## 1. Introduction

Porous manganese oxides are of considerable interest since these materials can be used in adsorption, catalysis, batteries, and other applications [1]. So far, micro- and mesoporous manganese oxides, as well as layered clay-like manganese oxide materials were prepared via a variety of routes. Among these materials, mesoporous manganese oxide has been the focus of intense interest for its nanoscale pore structure, high surface area and unique surface properties, which can reduce the solid-state diffusion distances and maximize the fraction of the interface to improve the electrochemical and catalytical behaviors of manganese oxides, especially when used as cathode material for lithium ion batteries [2].

Mesoporous manganese oxide with mixed-valent semiconducting property has been prepared from $Mn(OH)_2$ with cetyl trimethyl bromide(CTAB) surfactant as micellar template [3]. Novel

* Corresponding author. Tel.: +86-351-4044836; fax: +86-351-4040802.
*E-mail address:* hongxinlin@vip.sina.com (G. Zhang).

0025-5408/$ – see front matter © 2003 Elsevier Ltd. All rights reserved.
doi:10.1016/j.materresbull.2003.07.005

tetraalkylammonium manganese oxide colloids with a plate-like 4–12 nm in diameter have been synthesized from reduction of tetraalkylammonium permangate [4]. These colloids were prepared in a delaminated form and can undergo self-assembly to produce layered structure, showing a unique semiconducting property. Recently, Liu et al. succeeded in synthesizing a $SiO_2$-pillared birnessite using octylamine to preliminarily expand the layer structure and use tetraethoxylsilane (TEOS) as the pillaring source [5]. Their results showed evidence of the formation of a pillared mesoporous structure. Hong et al. prepared mesoporous manganese oxide using non-ionic surfactant (polyoxyethylene fatty alcohol, $AEO_9$) template in the sol–gel process of synthesizing cryptomelane [6]. BET surface area of the material is as high as 387 $m^2/g$, and its mesopore structure shows good thermal stability up to 500 °C in air.

Mesoporous manganese oxides have been obtained using a wide range of low temperature, liquid-phase methods, and these materials are excellent precursors for other functional materials. Sol–gel routes have been widely used in the synthesis of microporous (cryptomelane) and layered (birnessite) manganese oxides from reduction of $KMnO_4$ with organic reducing agents [7–9]. Little attention has been focused on the relationship of these sol–gel processes, resulting mesoporous aerogels and the colloidal suspensions derived from the synthesis.

Recently, synthesis and characterization of mesoporous manganese oxides via surfactant templating method were reported [6]. Meanwhile, the rheology of the suspensions obtained during preparation was also studied, and a unique oscillation behavior (apparent viscosity, storage modulus and loss modulus all fluctuate with gelation time) exists in these suspensions [10]. In the present work, we obtained mesoporous manganese oxides (MPMO) from reduction of $KMnO_4$ with maleic acid, and characterized this material in detail. The results show that MPMO is a pseudo-crystalline material with complex network pore structure, of which BET specific surface area is 297 $m^2/g$ and pore size distribution is approximately in the range of 0.7–6.0 nm. The MPMO material turns to cryptomelane when the calcinating temperature rises to 400 °C. Furthermore, systematic study on this sol–gel process indicated that the pore structures of manganese oxides synthesized are affected directly by several factors (molar ratio ($KMnO_4/C_4H_4O_4$), pH, gelating time).

## 2. Experimental

### 2.1. Sample preparation

MPMO was typically synthesized by mild reduction of aqueous solution of $KMnO_4$ with maleic acid at a molar ratio of $KMnO_4/C_4H_4O_4 = 3$ at room temperature. The resulting dark brown gel was kept at room temperature in air for 24 h and then filtered and washed with double deionized water for six times. After that, the gel was dried at 60 °C in air for about 20 h.

MPMO material was heated at 200, 300, 400 °C in air for 3 h, respectively. And the resultant corresponding samples were marked as MPMO-200, MPMO-300 and MPMO-400.

### 2.2. Characterization techniques

High-resolution transmission electron microscopy (HRTEM) was carried out using a JEM-2010 JEOL (Japan) ultra high-resolution microscope operated at 200 kV and 100 mA. Test samples were directly crushed and sprinkled onto carbon-coated grids (JEOL, Japan).

X-ray powder diffractometry (XRD) was performed at room temperature, using a Rigaku diffractometer equipped with a source of Ni-filtered Cu Kα radiation ($\lambda = 1.5406$ Å), and an X-ray generator operated at 40 kV and 100 mA. The diffractograms were recorded in the range of 10–80° with divergence and scaller slits of 1°, at a step size of 0.02° and a step time of 0.12 s.

The specific surface area and pore size distribution were determined by BET [11], *t*-plot [12], and BJH [13] analysis of $N_2$ adsorption–desorption isotherms measured on the samples, using automatic ASAP 2010 Micromeritics sorptometer (USA) equipped with an outgassing platform and on-line data acquisition and handling system. The nitrogen gas was a 99.999% pure product of PRAXAIR (Beijing, PR China), and the sample outgassing was carried out at 100 °C and $10^{-5}$ Torr for 5 h. The reproducibility of the measurements was better than 98%.

## 3. Results and discussion

### 3.1. Material characteristics

#### 3.1.1. Bulk properties

TEM micrographs obtained from MPMO (Fig. 1a–c) indicate that the material is a complex network pore structure. The selected area electron diffraction (SAED) (Fig. 1a) pattern accounts for a relatively pseudo-crystalline state (i.e. the microstructure of material is a mixture of orderly and disorderly regions). The HRTEM micrograph of MPMO (Fig. 1d) reveals that the test material consists of some layered domains.

The MPMO powders show nearly amorphous X-ray powder diffraction pattern (Fig. 1a), but some peaks are detected, such as 6.91, 3.65 Å. These parameters are similar to those of synthetic birnessite (OL-1) [9], indicating that there is some layered structure existing in MPMO. This is in accordance with the HRTEM observation above. Thermal treatment of MPMO at 400 °C leads to the formation of cryptomelane structure, whose XRD pattern is similar to that of [7]. After calcinating at 600 °C, the powders show sharp XRD pattern of cryptomelane with some peaks for bixbyite ($Mn_2O_3$, 3.85, 2.72 Å) emerged (Fig. 2c).

MPMO is a mixture of layered and disordered domain, and the transition of layered structure to cryptomelane have not been reported in other manganese oxide materials sol–gel synthesized via reduction of $KMnO_4$ with maleic acid [7]. The similar conversion is just mentioned in the work of spontaneous formation of manganese oxide helices [14], which is prepared from reduction of tetramethyl ammonium permanganate with 2-butanol/$H_2O$.

#### 3.1.2. Pore structure

$N_2$ adsorption–desorption isotherm (Fig. 3a) of MPMO belongs to BDDT type IV, indicating that the test material expose mesoporous structure. The hysteresis loop in the isotherm is similar to type-H2, which is associated with a more complex network pore structure [15]. This result is supported by directly HRTEM observation of MPMO (Fig. 1). The BET surface area is 297 $m^2/g$ (Table 1), and pore size distribution derived from the desorption branch is between 1.7 and 6.0 nm (Fig. 3a). The *t*-plot curve for sample (Fig. 3b) shows a downward deviation to the straight line from around 0.7 nm, due to micropore filling of nitrogen. This indicates that micropores with width around 0.7 nm exist in MPMO, i.e. the layered structures observed from HRTEM and XRD. Meanwhile, *t*-plot analysis gives a

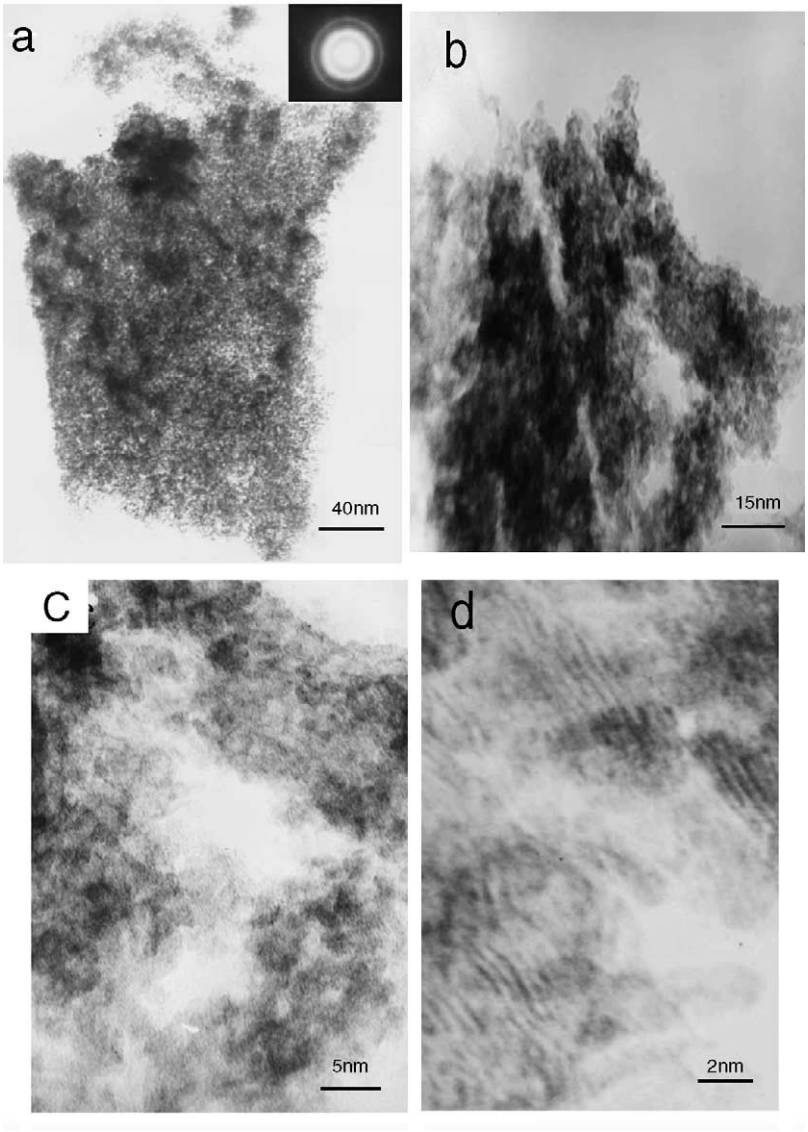


Fig. 1. HRTEM photographs of MPMO materials.

Table 1
Pore properties of samples treated at different temperature

| Sample | $S_{BET}$ ($m^2/g$) | $C_{BET}$ | $S_{mp}$ ($m^2/g$) | $S_{ext}$ ($m^2/g$) | $V_{de}$ ($cm^3/g$) | $D_{de}$ (nm) |
|---|---|---|---|---|---|---|
| MPMO | 297 | 161 | 33 | 264 | 0.277 | 3.59 |
| MPMO-200 | 313 | 196 | 57 | 256 | 0.279 | 3.62 |
| MPMO-300 | 235 | 148 | 21 | 213 | 0.252 | 3.72 |
| MPMO-400 | 43 | 291 | 9 | 34 | 0.125 | 10.38 |

$S_{mp}$: surface area of micropore; $S_{ext}$: surface area of external surface; $V_{de}$: pore volume calculated from desorption branch; $D_{de}$: average pore diameter calculated from desorption branch and referred to mean hydraulic diameter $D_p = 4V_p/S_p$.

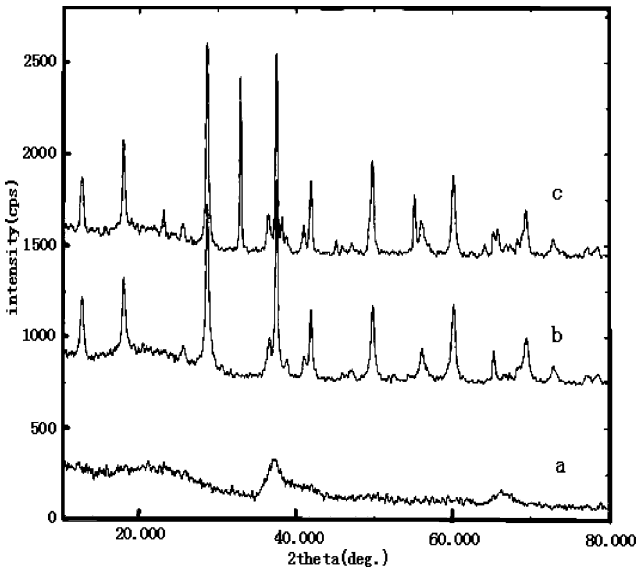


Fig. 2. XRD patterns of samples. (a) MPMO, (b) MPMO-400, (c) MPMO-600.

micropore surface area ($S_{mp}$) of 33 $m^2/g$ and external surface area ($S_{ext}$) of 264 $m^2/g$. This means that the layered plates stack irregularly to form abundant mesopores.

Fig. 4 shows the $N_2$ adsorption results of samples treated at different temperature. It proves that the pore structure of MPMO material is stable to calcination up to 300 °C, because of the similar isotherms and hysteresis loops of MPMO, MPMO-200 and MPMO-300 (Fig. 4a). With temperature increasing, the two peaks of MPMO's pore size distribution curve (Fig. 4b) exhibit different changes, one (around 3.2 nm) increases, and the other (around 5.0 nm) decreases. The enhanced peak is due to exposure of new pores, which were occupied by water and oxalic acid molecules before thermal treatment. At the same time, the peak (around 5.0 nm) decreased, because larger pores of MPMO readily collapse during calcination.

The pore properties of samples treated at different temperature are shown in Table 1. It indicates that this kind of irregularly stacked mesopore can withstand thermal treatment up to 300 °C. The $C_{BET}$ constants are below 200 at lower 400 °C. Because $C_{BET}$ value is a measure of the strength of interaction between the nitrogen molecule and pore surface, the low $C_{BET}$ value indicates the weak interaction between the nitrogen molecule and pore surface due to the presence of relatively wide mesopore structures. At 400 °C, $C_{BET}$ constant is 291, this is attribute to the formation of cryptomelane, in which a typical 4.6 Å tunnel structure is in existence.

### 3.2. Sol–gel process

MPMO of high surface area is good precursor for preparing different functional materials, which can be used in electrochemistry, catalysis, sensors, etc. The sol–gel process for MPMO is very sensitive to variations in reaction conditions, and the resulting material is quite different in structure and properties. Here, BET surface area was chosen as the main parameter to scale the relationship between the pore structure and several reaction factors of the sol–gel process.

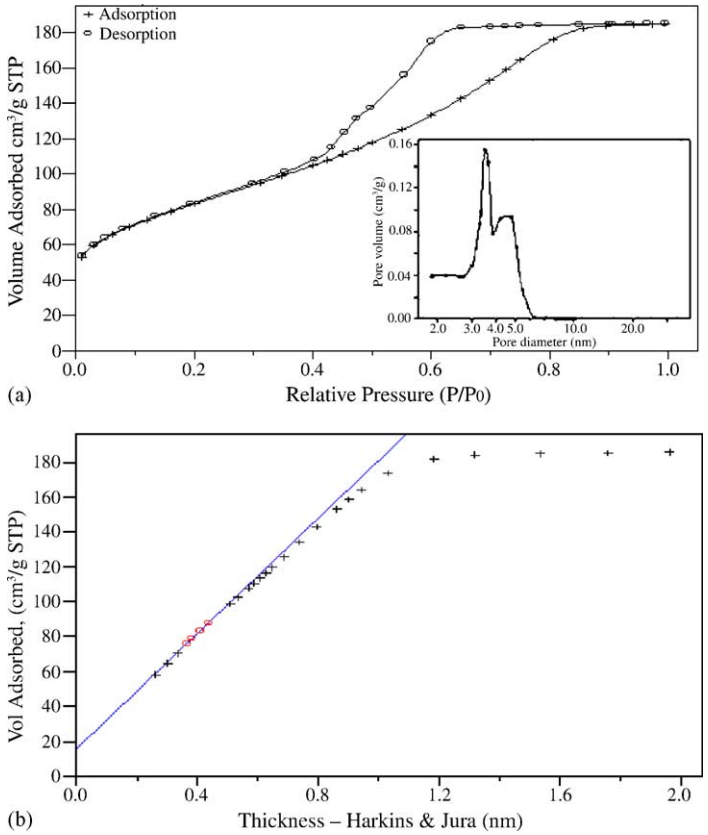


Fig. 3. $N_2$ adsorption–desorption results of MPMO material. (a) $N_2$ adsorption–desorption isotherm and pore size distribution curve, (b) *t*-plot curve.

### 3.2.1. $KMnO_4/C_4H_4O_4$ molar ratio

Results of sol–gel reactions with different molar ratio of $KMnO_4$ and maleic acid are shown in Fig. 5. Surface area of resulting sample reaches the highest at about 3. This can be easily understood to take this sol–gel mechanism [16,17] into account:

$$3HOOCCH{=}CHCOOH + 10MnO_4^- + 10H_3O^+ \rightarrow 10MnO_2 + 18H_2O + 6CO_2 + 3C_2O_4H_2$$

Following this mechanism, the optimum stoichiometry is $KMnO_4/C_4H_4O_4$ molar ratio $= 10/3 \approx 3.33$. Around this point, the sol–gel process is more complete and the attained network structure is more thoroughly organized. Because there are enough cross-linking molecules ($C_2O_4H_2$) to interconnect the manganese oxide centers, this is important for building the network mesopore. As a consequence, less maleic acid (high $KMnO_4/C_4H_4O_4$ molar ratio) leads to a quicker decrease in surface area.

### 3.2.2. pH effect

The initial pH value (adjusted with $H_2SO_4$ and KOH solution) of the solution affects directly the pore structure of manganese oxide obtained (Fig. 6). For the construction of mesoporous manganese oxide, it is better without any acid or base added into the starting solution. An increase in basicity accelerates gelation, but does not improve the $S_{BET}$ of the products. This is due to the reaction of cross-linking

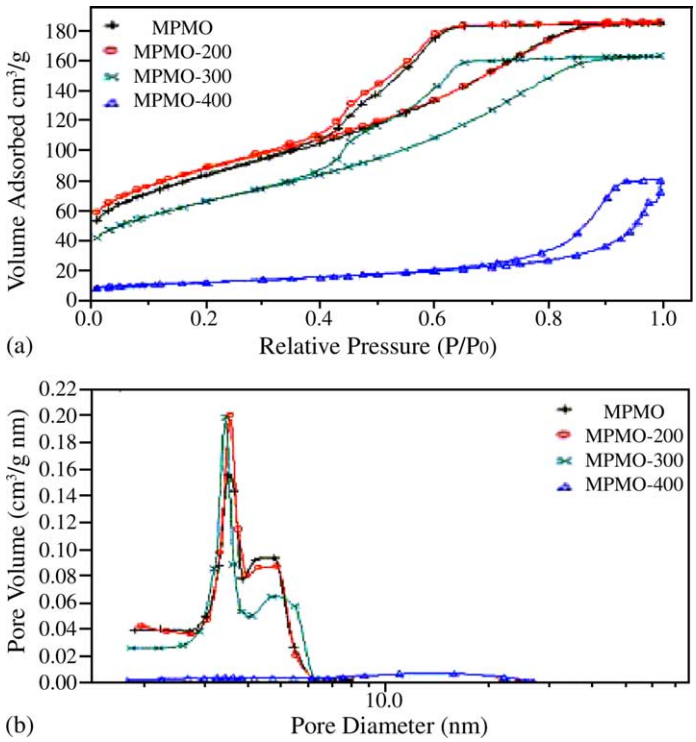


Fig. 4. $N_2$ adsorption–desorption results of samples treated at different temperature. (a) $N_2$ adsorption–desorption isotherms, (b) pore size distribution curves.

molecules (oxalic acid) with base, which breaks up the network structure. When acidity of the initial solution increases, the nature of the reaction changes from sol–gel to precipitation type. Because the electrical double layer of the colloidal particle surface is depressed strongly with the addition of acid, this reduces the electrostatic repulsive force produced by negative charges of colloidal surfaces, and is harmful to the formation of manganese oxide gel structure.

### *3.2.3. Gelation time*

Gelation is important for the sol–gel process to attain MPMO material of high surface area. Fig. 7 describes the time dependence of resulting pore structure. The result shows that the surface area of sample is nearly constant, when gelating after 6 h. After 1 h of stirring rapidly, the colloidal dispersion of manganese oxide begins to flocculate to form a continuous gel structure instead of individual flocs.

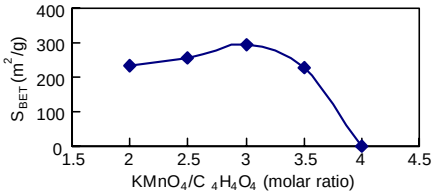


Fig. 5. $KMnO_4/C_4H_4O_4$ molar ratio effect on surface area of manganese oxides.

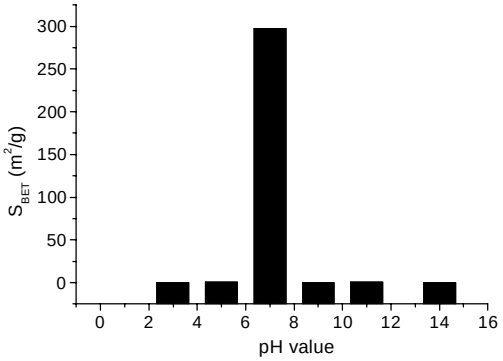


Fig. 6. pH effect on surface area of manganese oxides.

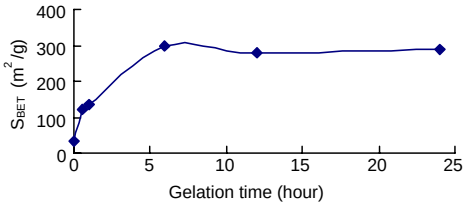


Fig. 7. The relationship of gelation time and the surface area of manganese oxides.

The gel structures build up slowly with time, as the particles orient themselves towards positions of minimum free energy under the influence of Brownian motion. The surface area of materials stays about the same after 6 h and suggests that the gel microstructure is complete.

From the discussion above, optimum reaction conditions to synthesize MPMO material of high surface area can be concluded, i.e. $KMnO_4/C_4H_4O_4$ molar ratio = 3, pH = 7 and gelation time > 6 h.

## 4. Conclusions

A simple sol–gel route has been developed for preparing MPMO with high surface area (297 $m^2$/g), of which pore distribution is locating at 0.7–6.0 nm. HRTEM, XRD and $N_2$ sorptometry were used to characterize this material, and the results showed that MPMO is a pseudo-crystalline material with complex network pore structure. The material can withstand thermal treatment up to 300 °C and turns to cryptomelane when the calcinating temperature rises to 400 °C. The effects of molar ratio ($KMnO_4/C_4H_4O_4$), pH value and gelating time on the pore structure of MPMO were also discussed in detail, and the optimum sol–gel reaction conditions is that $KMnO_4/C_4H_4O_4$ molar ratio = 3, pH = 7 and gelation time > 6 h.

## Acknowledgements

This research was funded by Fundamental Research Item (No. 2001ccc01300) of Technology Ministry of China. The authors would like to thank Surfactant Key Lab of China Research Institute of Daily Chemical Industry for its support.

## References

[1] S.L. Brock, N. Duan, Z.R. Tian, O. Giraldo, H. Zhou, S.L. Suib, Chem. Mater. 10 (1998) 2619.
[2] J.W. Long, R.M. Stroud, D.R. Rolison, J. Non-Crystalline Solids 285 (2001) 288.
[3] Z.R. Tian, W. Tong, T.Y. Wang, N.G. Duan, V.V. Krishnan, S.L. Suib, Science 276 (1997) 926.
[4] S.L. Brock, M. Sanabria, S.L. Suib, V. Urban, P. Thiyagarajan, D.I. Potter, J. Phys. Chem. B 103 (1999) 7416.
[5] Z.-H. Liu, K. Ooi, H. Kanoh, W. Tang, X. Yang, T. Tomida, Chem. Mater. 13 (2001) 473.
[6] X. Hong, G. Zhang, Y. Zhu, H. Yang, in: Proceedings of the 7th International Conference on Surfactants & Detergents, Shenzhen, China, 2002.
[7] N. Duan, S.L. Suib, C.-L. O'Young, J. Chem. Soc. Chem. Commun. (1995) 1367.
[8] S. Ching, J.L. Roark, N. Duan, S.L. Suib, Chem. Mater. 9 (1997) 750.
[9] S. Ching, D.J. Petrovay, M.L. Jorgensen, S.L. Suib, Inorg. Chem. 36 (1997) 883.
[10] X. Hong, G. Zhang, Y. Zhang, Y. Zhu, H. Yang, Acta Chim. Sinica 60 (2002) 1872–1875.
[11] S. Brunauer, P.H. Emmett, E. Teller, J. Am. Chem. Soc. 60 (1938) 309.
[12] A.J. Lecloux, in: J.R. Anderson, M. Boudart (Eds.), Catalysis-Science and Engineering, vol. 2, Springer, Berlin, 1981, p. 171.
[13] P.E. Barrett, L.S. Joynor, P.P. Halenda, J. Chem. Soc. (1951) 373.
[14] O. Giraldo, S.L. Brock, M. Marquez, S.L. Suib, H. Hillhouse, M. Tsapatsis, Nature 405 (2000) 38.
[15] K.S.W. King, J. Rouquerol, in: G. Ertl, H. Knözinger, J. Weitkamp (Eds.), Handbook of Heterogeneous Catalysis, vol. 2, Wiley-YCH, Weinhein, 1997, p. 427.
[16] M. Jaky, L.I. Simandi, L. Mavos, I. Molnar-Perl, J. Chem. Soc., Perkin Trans. 2 (1973) 1565.
[17] L.I. Simandi, M.J. Jaky, Chem. Soc. Perkin Trans. 2 (1973) 1856.